Published February 3, 2015

Hydropedology Symposium: 10 Years in the Past and 10 Years into the Future

Mapping of Hydropedologic Spatial Patterns in a Steep Headwater Catchment

Cody P. Gillin
Dep. of Forest Resources and Environmental Conservation
Virginia Tech
Blacksburg, VA 24061

current address:
Trout Unlimited
103 Palouse Street, Suite 14
Wenatchee, WA 98801

Scott W. Bailey*
US Forest Service
Northern Research Station
234 Mirror Lake Road
North Woodstock, NH 03262

Kevin J. McGuire
Virginia Water Resources Research Center
and
Dep. of Forest Resources and Environmental Conservation
Virginia Tech
Blacksburg, VA 24061

John P. Gannon
Geosciences and Natural Resources Dep.
Western Carolina Univ.
Cullowhee, NC 28723

A hydropedologic approach can be used to describe soil units affected by distinct hydrologic regimes. We used field observations of soil morphology and geospatial information technology to map the distribution of five hydropedologic soil units across a 42-ha forested headwater catchment. Soils were described and characterized at 172 locations within Watershed 3, the hydrologic reference catchment for the Hubbard Brook Experimental Forest, New Hampshire. Soil profiles were grouped by presence and thickness of genetic horizons. Topographic and bedrock metrics were used in a logistic regression model to estimate the probability of soil group occurrence. Each soil group occurred under specific settings that influence subsurface hydrologic conditions. The most important metrics for predicting soil groups were Euclidean distance from bedrock outcrop, topographic wetness index, bedrock-weighted upslope accumulated area, and topographic position index. Catchment-scale maps of hydropedologic units highlight regions dominated by lateral eluviation or lateral illuviation and show that only about half the catchment is dominated by podzolization processes occurring under vertical percolation at the pedon scale. A water table map shows the importance of near-stream zones, typically viewed as variable source areas, as well as more distal bedrock-controlled zones to runoff generation. Although the catchment is steep and underlain by soils developed in coarse-textured parent material, patterns of groundwater incursion into the solum indicate that well-drained soils are restricted to deeper soils away from shallow bedrock and the intermittent stream network. Hydropedologic units can be a valuable tool for informing watershed management, soil C accounting, and understanding biogeochemical processes and runoff generation.

Abbreviations: AIC, Akaike information criterion; DEM, digital elevation model; DI, downslope index; EAS, elevation above stream; EDb, Euclidean distance from bedrock outcropping; EDs, Euclidean distance from stream; Elev, elevation; FDs, flow distance from stream; HBEF, Hubbard Brook Experimental Forest; HPU, hydropedologic unit; LiDAR, light detection and ranging; MNR, multinomial logistic regression; NMS, nonmetric multidimensional scaling; PLAN, planform curvature; PROF, profile curvature; SLP, slope; TPI, topographic position index; TWId, topographic wetness index using downslope index; TWIs, topographic wetness index using slope; UAA, upslope accumulated area; UAAb, bedrock-weighted upslope accumulated area; WS3, Watershed 3.

Topography and hydrologic processes were long ago recognized as key factors affecting soil development (Jenny, 1941; Bushnell, 1943). Hillslope shape influences water flow through soils and has been linked with soil variability and development (e.g., Pennock et al., 1987; Moore et al., 1993). Recently, it has been suggested that interdisciplinary approaches combining expertise from hydrology, pedology, and geomorphology, and emphasizing structure

Soil Sci. Soc. Am. J.
doi:10.2136/sssaj2014.05.0189
Received 8 May 2014.
Accepted 20 Nov. 2014.
*Corresponding author (swbailey@fs.fed.us).
© Soil Science Society of America, 5585 Guilford Rd., Madison WI 53711 USA
All rights reserved. No part of this periodical may be reproduced or transmitted in any form or by any means, electronic or mechanical, including photocopying, recording, or any information storage and retrieval system, without permission in writing from the publisher. Permission for printing and for reprinting the material contained herein has been obtained by the publisher.

and pattern to formulate hypotheses about system function, are critical to advancing our understanding of hydrologic processes (McDonnell et al., 2007). The emerging discipline of hydropedology, or the integration of hydrology and soil science (Lin et al., 2006), provides a useful framework for examining soil spatial patterns in headwater catchments that offers insight into hydrologic dynamics and biogeochemical processes. The linkage between controls on flow pathways and soil development provides unique opportunities for mapping soils that consider the role of water in soil development at pedon to hillslope scales.

During the past two decades, technological advancements have facilitated an evolution of digital soil mapping approaches (Lagacherie et al., 2006; Boettinger et al., 2010). Soils can be represented as discrete units with sharp boundaries or as fuzzy units with gradual transitions, which may better reflect the continuous variations present in soils. In addition, raster-based maps can differentiate small areas of distinct soil traditionally considered as unmapped inclusions in polygon-based map units derived using standard soil survey approaches. Uncertainty can also be conveyed using fuzzy representations, which permit membership of more than one soil type for each mapped unit and result in gradual transitions between soil units. Categorization, based on probability ranging from 0 (no confidence) to 1 (full confidence), can be used to assign fuzzy membership. One fuzzy approach to digital soil mapping involves logistic regression modeling using terrain variables to predict soil class probabilities (Debella-Gilo and Etzelmuller, 2009). Unlike multiple linear regression, logistic regression is less demanding in terms of data characteristics such as normality, linearity, and equal variance of independent variables, and in particular it accommodates nonlinear relationships in soil–landscape associations (Bailey et al., 2003b).

Although previous studies have demonstrated the utility of logistic regression as a quantitative approach to digital soil mapping, most made predictions using coarse digital elevation models (DEMs) of 25 m or greater grid size (e.g., Kempen et al., 2009). Recently, high-resolution DEMs (1–10 m) derived from light detection and ranging (LiDAR) data have become more accessible, and their use for topographic analysis and topographic metric computation is increasingly commonplace. In pedogenic and geomorphologic applications, such topographic analyses are often used as surrogates for the spatial variation of hydrologic processes and conditions such as different soil moisture conditions and flow patterns (Merot et al., 1995; Guntner et al., 2004) and thus may be useful for understanding soil variation as influenced by the hydrologic condition (Gessler et al., 2000; Brown et al., 2004; Seibert et al., 2007).

The relationships among landscape, water, and soil have been critical components of biogeochemical research at the Hubbard Brook Experimental Forest (HBEF) (e.g., McDowell and Wood, 1984; Johnson et al., 2000; Palmer et al., 2004; Zimmer et al., 2013). Soils at the HBEF have been characterized as well-drained Spodosols with considerable spatial heterogeneity of physical and chemical properties (Huntington et al., 1988; Johnson et al., 2000), yet spatial averaging in soil investigations at the pedon scale to evaluate catchment-scale ecosystem processes is common and does not allow an understanding of how soil spatial organization influences ecosystem processes (Bailey et al., 2014). More recent investigations have shown the frequent occurrence of transient water tables (Detty and McGuire, 2010) in steep upland catchments where the groundwater has been thought to not have an important role in catchment biogeochemical processes (Likens and Buso, 2006; Likens, 2013). Differences in the frequency and duration of water table incursions in the solum (i.e., the soil profile above the C horizon) in various portions of the catchment lead to distinct soil horizonation patterns and underscore the influence of downslope hydrologic flow on podzolization at the pedon to hillslope scales (Bailey et al., 2014; Gannon et al., 2014; Bourgault et al., 2015).

Field examination of soil morphological differences in Watershed 3 (WS3), one of the HBEF reference watersheds, led to the conceptualization of functional soil units reflecting distinctive hydrologic regimes (Bailey et al., 2014; Fig. 1). Focus on the pedon as the unit of soil study may lead to an overemphasis on water and solute transport and soil development as vertical in nature (Zaslavsky and Rogowski, 1969), yet many studies have documented lateral components to water flow through soils (McDaniel et al., 1992) affecting podzolization (Sommer et al., 2000; Jankowski, 2013) and pedogenic processes in general (Sommer and Schlichting, 1997; Park and Burt, 2002). In steep topography or mountainous regions where subsurface heterogeneities or relatively shallow bedrock facilitate lateral water movement, soil development patterns result in translocational catenas at the hillslope scale (Sommer et al., 2000; Bailey et al., 2014). Better recognition of lateral translocation of clays, organic acids, and dissolved metals could provide the basis for enhanced understanding of hydrologic, pedogenic, and biogeochemical processes and patterns at various scales from the pedon to the catchment.

Hydropedologic functional units (Lin et al., 2008) have been suggested as an alternative method for mapping soils, with units based on soils of similar pedologic and hydrologic functions. In practice, these have been mapped by subdividing standard soil-series-based map units by variations in specific soil properties, such as surface horizon texture or depth to a clay layer, that are important to the hydrologic response (Zhu et al., 2013). The research at HBEF has developed differently because no detailed soil survey is available and the development of hydropedologic units (HPUs) was made independently of established soil series.

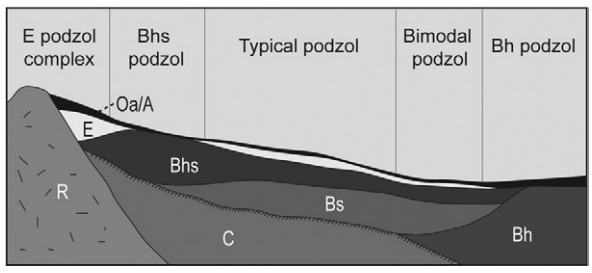

Fig. 1. Conceptual representation of five hydropedologic units along an idealized hillslope toposequence (modified after Bailey et al., 2014).

Rather, this was simply an attempt to describe the spatial variation in the soil horizon sequences observed, hypothesizing that these variations were due to differences in hydrologic regimes in different portions of a watershed (Bailey et al., 2014). This hypothesis has stood up to analyses of the temporal variation in water table fluctuations (Gannon et al., 2014) and micromorphological and chemical differences in spodic horizons (Bourgault et al., 2015). Thus the concept of an HPU is somewhat different from a hydropedologic functional unit sensu Lin et al. (2008) and has been defined as "a grouping of variations in soil morphology that directly relate influence of water table regime, flow paths, and saturation to soil development" (Gannon et al., 2014).

Such an approach of mapping HPUs emphasizes hydrologic controls on soil development and material transfer between soil units along hydrologic catenas. If hillslope shape and position affect hydrologic processes that in turn influence soil development, then topographic information should be useful in interpreting hydrologic processes and predicting soil attributes and soil morphological variation. This study aimed to apply digital soil mapping techniques using topographic metrics computed from a high-resolution DEM to predict the spatial distribution of HPUs across a 42-ha headwater catchment at the HBEF. We propose that mapping HPUs will facilitate a better understanding of catchment functionality in terms of hydrology, biogeochemistry, soil quality, and management concerns such as forest nutrition and soil C storage.

METHODS

Study Location

The HBEF (Fig. 2), located in the White Mountains of New Hampshire (43°56′ N, 71°45′ W), is maintained by the US Forest Service, Northern Research Station, and is part of the National Science Foundation Long-Term Ecological Research network. The experimental watersheds, including WS3, the hydrologic reference catchment, are underlain by mica schist and calc-silicate granulite of the Silurian Rangeley formation (Barton et al., 1997) and mostly covered by Wisconsinan glacial drift of varying thickness, primarily composed of granitic rocks (Bailey et al., 2003c). Soils are predominantly Spodosols of sandy loam to loamy sand texture developed in glacial drift parent materials (Bailey et al., 2014). Elevation ranges from 527 to 732 m. The western side of the catchment is characterized by spurs flanking intermittent and perennial streams, whereas the eastern portion exhibits less dissected topography and less well developed stream channels (Fig. 3). Bedrock outcrops are most common along the ridge crests and the middle to upper portions of catchment boundaries.

Climate at the HBEF is humid continental. Winters tend to be long and cold, with an average January temperature of −9°C. Summers are mild, with July temperatures averaging 19°C (temperature averages recorded at 450-m elevation). Annual precipitation averages 1400 mm, with about 30% falling as snow (Bailey et al., 2003a).

The catchment is dominated by second-growth northern hardwood forest including sugar maple (*Acer saccharum* Marshall), American beech (*Fagus grandifolia* Ehrh.) and yellow birch (*Betula alleghaniensis* Britton), with shallow-to-bedrock areas dominated by red spruce (*Picea rubens* Sarg.) and balsam fir [*Abies balsamea* (L.) Mill.] interspersed with mountain white birch (*Betula cordifolia* Regel). The forest was partially harvested between 1870 and 1920, damaged by a hurricane in 1938, and is not currently aggrading (Siccama et al., 2007; Likens, 2013).

Soil Characterization

The study site is in a glaciated upland that has been described as a catena of Lyman–Tunbridge–Becket series, with well-drained Spodosols of increasing depth from bedrock-dominated ridges to lower slopes with thicker glacial drift (Huntington et al., 1988; Homer, 1999). Five HPUs (E, Bhs, typical, bimodal, and Bh podzols) displaying distinct horizonation, a range of podzolization, and variation in the frequency and duration of transient groundwater saturation in the solum have been observed and described in WS3 (Fig. 1; Bailey et al., 2014). The E podzols had an E horizon up to 40 cm thick and minimal or absent B horizon overlying a C horizon or bedrock. The E podzols occur in bedrock-controlled landscapes near the watershed divide where water tables rise into the solum for brief periods during rainfall events throughout the year. They are often interspersed with bedrock outcrops covered by mosses and lichens as well as Histosols in pockets of organic accumulation in bedrock depressions and outcrops. Together, these assemblages of E podzols, shallow Histosols, and bedrock outcrops are referred to as an E podzol complex (Fig. 1). The Bhs podzols are

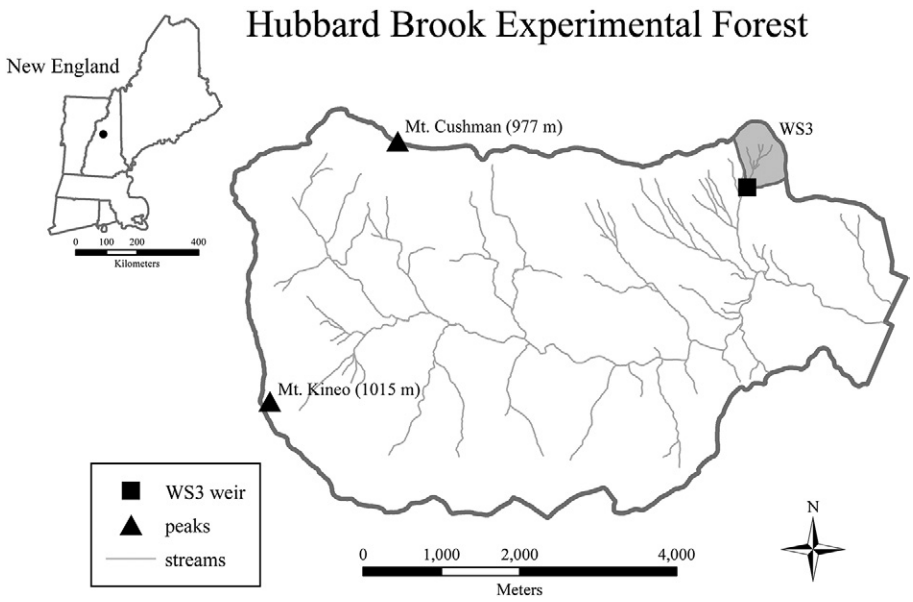

Fig. 2. Map of Hubbard Brook Experimental Forest, Watershed 3, and location within New England, United States.

found downslope and adjacent to E podzols, with similar flashy water table response on an event basis but with a longer recession than the E podzols (Gannon et al., 2014). The Bhs podzols tend to lack an E horizon but have an unusually thick Bhs horizon, up to 54 cm thick, that dominates the solum. The E and Bhs podzols are similar to the lateral podzols discussed by Sommer et al. (2000). Typical podzols best fit the established soil series for the region (Homer, 1999; Bailey et al., 2014), with thin and discontinuous E horizons overlying a sequence of Bhs and Bs horizons. Typical podzols comprise the majority of soils sampled in WS3 and are most commonly found on backslopes throughout the catchment. Groundwater monitoring in typical podzols shows infrequent incursions in the lower portion of the solum, suggesting that vertical unsaturated percolation is the dominant hydrologic process influencing soil development of this unit (Bailey et al., 2014; Gannon et al., 2014). Bimodal podzols are a transitional unit found at backslope to footslope positions downslope of typical podzols. These soils have an upper sequence resembling that of a typical podzol but also contain a Bh horizon of darker illuviated spodic material at the B–C interface (Bourgault et al., 2015), where water tables rise into the lower solum seasonally and during events. The Bh podzols occur on topographic benches, swales, and in particular at streamside locations and are most influenced by saturated flow during frequent water table incursions into the solum during larger events in the summer and throughout the non-growing season (Bailey et al., 2014; Gannon et al., 2014). They are comprised of thick, dark Bh horizons for the majority of the solum and typically lack an E horizon.

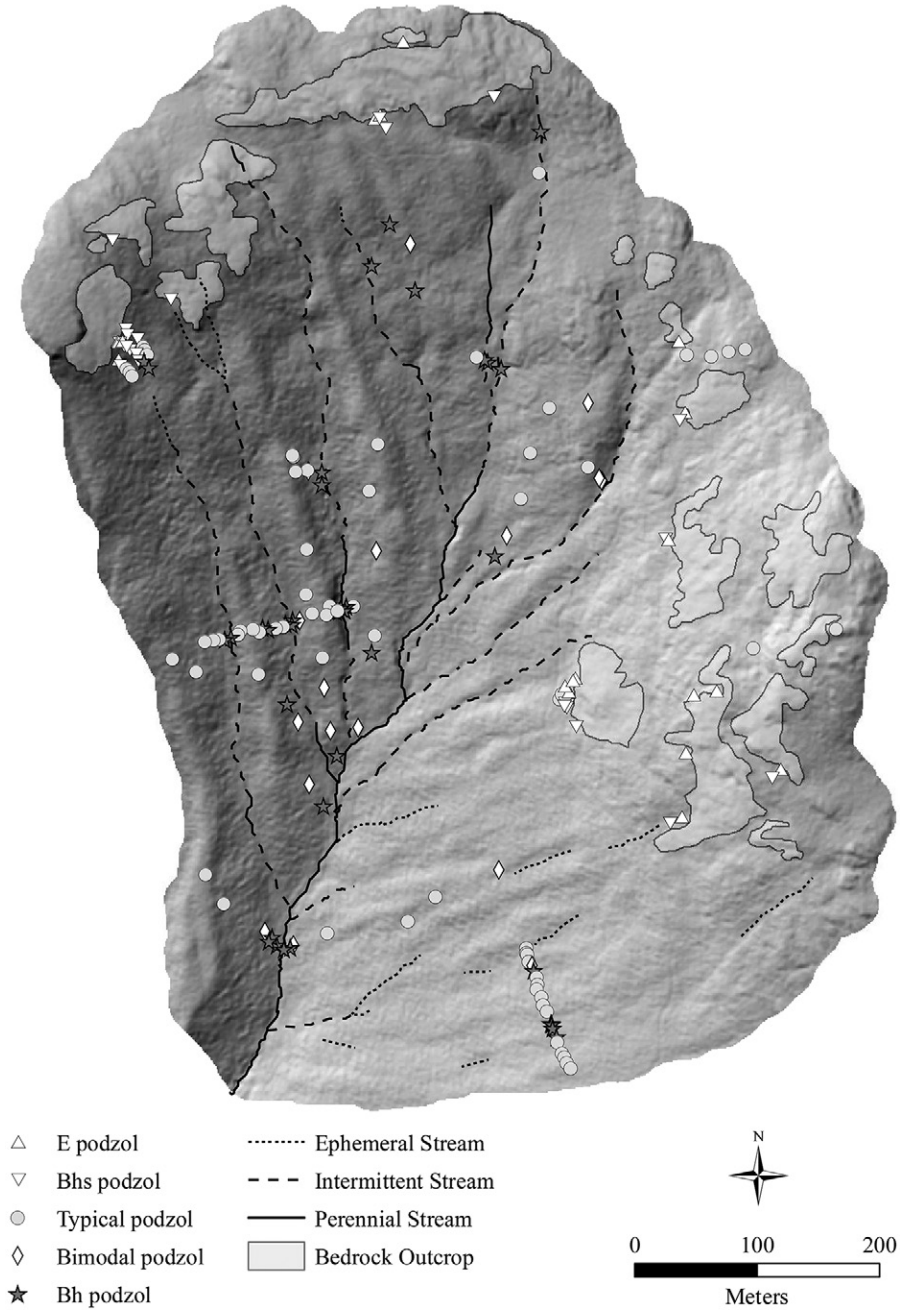

Fig. 3. Map of soil pits, streams, and bedrock outcrops. A total of 172 soil pits were located in Watershed 3. Soil characteristics, including horizon thicknesses, Munsell color values, and texture, were used to designate genetic soil horizons and infer the hydropedologic unit. Light gray areas represent regions where bedrock is at or near the surface.

Although defined somewhat differently in the U.S. soil taxonomy, Bailey et al. (2014) used a field designation of Bh for horizons with predominately a 10YR hue and a value and chroma of 3/3 or less in contrast to Bhs and Bs horizons that had a hue of 7.5YR or redder. Bourgault et al. (2015) showed that these horizons designated as Bh had a chemistry and morphology distinct from Bhs and Bs horizons in typical podzols. The Bh horizons are found in bimodal and Bh podzols without an overlying E horizon but where the associated eluvial horizon is some distance upslope on the hillside.

A total of 172 hand-dug soil pits were described between 2008 and 2012 (Fig. 3). Fifty-nine soil sampling sites from Bailey et al. (2014) were included in this data set, and additional locations were selected to include the range of topographic and landscape positions in the catchment. Earlier sampling sites were positioned singly or along transects of three to six pits along hillslopes. In the present study, intensive transects and grids at 3- to 10-m intervals were sampled across landforms and adjacent bedrock outcrops to document fine-scale soil morphological changes and transitions between HPUs. Each profile was described by horizon presence, depth, and color to designate genetic horizons and then assigned to an HPU based on

the presence and relative thickness of soil horizons (Bailey et al., 2014). Locations for each pit were determined using a Trimble Geo XT 2005 GPS unit equipped with a Trimble Hurricane Antenna. Data were differentially corrected using Trimble Pathfinder software and Continuously Operating Reference Station (CORS) data from the National Geodetic Survey to obtain approximately 1-m precision of horizontal positions.

LiDAR Data Collection and Topographic Metric Computation

The LiDAR data were collected for the White Mountain National Forest in April 2012 by Photo Science, Inc., during leaf-off and snow-free conditions. Points classified as ground were used to interpolate a 1-m DEM using Terrasolid (www.terrasolid.com). Ground return densities in WS3 were determined to be approximately 1.16 points m^{-2}.

We coarsened and filtered the 1-m DEM through mean cell aggregation to a 5-m grid resolution. Calculation of the upslope accumulated area and topographic wetness index were found to be sensitive to DEM resolution, and the 5-m resolution best captured a range in these parameters that corresponded with the scale of landforms present in the catchment (Gillin et al., 2015). The DEM was treated with a low-pass smoothing filter over a nine-cell square neighborhood moving window to remove high-frequency data. A sink-filling algorithm (Wang and Liu, 2006) was applied to the DEM to maintain the downslope gradient and facilitate the computation of topographic metrics related to flow.

Numerous topographic metrics were computed from the filtered and filled DEM (Table 1) using ArcMap Version 10.1 and the System for Automated Geoscientific Analyses (SAGA) (Conrad, 2011). Two slope parameters were calculated: the first (SLP) was calculated using the maximum slope algorithm (Travis et al., 1975) and the second (DI) using the downslope index (DI = d/L_d, where L_d is the horizontal distance to a point with an elevation d meters below the elevation of the starting cell following the steepest direction flow path [Hjerdt, 2004]). A value of 5 m was used for this analysis. The upslope accumulated area (UAA) was computed using the triangular multiple flow direction algorithm (Seibert and McGlynn, 2007). Subsequently, two versions of the topographic wetness index [TWI = $\ln(a/\tan\beta)$, where a is the UAA and $\tan\beta$ is the local slope (Beven and Kirkby, 1979)] were computed. The TWIs used the maximum slope (SLP) for $\tan\beta$ and TWId used the DI for $\tan\beta$. A single direction flow algorithm was used to compute the flow distance (FDs) from every cell to its drainage point on the stream network. Planform (PLAN) and profile (PROF) curvature were determined using the method of Zevenbergen and Thorne (1987). A topographic position index (TPI) was calculated by the difference between the elevation of each cell and the mean elevation for a neighborhood of cells in a moving circular window of 100-m radius centered on the target cell (Guisan et al., 1999). Positive values of TPI were generally associated with summit and shoulder positions, while negative values were associated with footslopes and toeslopes. Other geographic variables were computed including the Euclidean distance from stream channels (EDs) and bedrock (EDb).

A map of the portion of the watershed dominated by bedrock outcrops was made by visual inspection while walking transects and outcrop perimeters with a handheld GPS unit (Fig. 3). The potential influence of outcrops and shallow bedrock regions on the soil distribution was included as a new topographic metric of bedrock-weighted UAA (UAAb). For any location in the catchment, this metric expresses the relative influence of bedrock outcrops and shallow bedrock regions in the UAA draining to that location. The UAAb metric was calculated using the

Table 1. Topographic metrics evaluated for predicting soil group spatial distribution and Spearman correlation with ordination of presence or absence of genetic soil horizons and soil horizon thickness data using nonmetric multidimensional scaling (NMS).

			Spearman correlation†		
Metric	Variable	Reference	NMS 1	NMS 2	NMS 3
Raw elevation (m)	Elev		0.32***		0.32***
Slope (%)	SLP	Travis et al. (1975)	0.21**		
Downslope index (%)	DI	Hjerdt (2004)	0.21**		
Planform curvature	PLAN	Zevenbergen and Thorne (1987)	0.26***		
Profile curvature	PROF	Zevenbergen and Thorne (1987)			−0.29***
Elevation above stream (m)	EAS	SAGA‡	0.36***		
Euclidean distance from stream (m)	EDs	ArcMap 10.1	0.45***	0.25**	0.22**
Flow distance from stream (m)	FDs	ArcMap 10.1	0.40***		0.21**
Euclidean distance from bedrock (m)	EDb	ArcMap 10.1	−0.34***		−0.46***
Topographic wetness index [$\ln(m^2)$]	TWIs	Beven and Kirkby (1979)	−0.35***		
Topographic wetness index (downslope) [$\ln(m^2)$]	TWId	Hjerdt (2004)	−0.35***		
Upslope accumulated area (m^2)	UAA	Seibert and McGlynn (2007)	−0.35***		0.16*
Bedrock-weighted upslope accumulated area	UAAb	this study	0.20**		0.44***
Topographic position index (m)	TPI	Guisan et al. (1999)	0.28***	0.31***	

* $p < 0.05$.

** $p < 0.01$.

*** $p < 0.001$.

† Spearman correlations are provided for each of the NMS axes. Only correlations with $p < 0.05$ are shown.

‡ System for Automated Geoscientific Analyses (Conrad, 2011).

triangular multiple flow direction accumulated area algorithm (Seibert and McGlynn, 2007) within SAGA using a weighting grid. The weighting grid was created by assigning large weight values (10^5) to all bedrock outcrop cells and a zero weight to all other cells. The ratio of the weighted UAA to the unweighted UAA was normalized so that it varied between 0 and 1 and values closer to 1 had the highest proportions of bedrock in the upslope area. This normalized ratio of the weighted UAA to the unweighted UAA is the UAAb.

Ordination of Soil Data Using Nonmetric Multidimensional Scaling

The distinctness of the HPUs and their relationship to topographic metrics was examined using a nonmetric multidimensional scaling (NMS) ordination of the thickness of the genetic soil horizons at each sampling pit. We selected the Bray–Curtis dissimilarity (Bray and Curtis, 1957) as the measure of distance in the ordination space because it has been shown to be useful in the analysis of nonlinear ecological gradients (Faith et al., 1987). We examined the ordination of HPU data in both two and three dimensions to determine the number of dimensions required to reduce Kruskal's stress criterion (Clarke, 1993). Finally, a biplot of the topographic metrics, represented by Spearman correlates (vectors), was placed over the NMS ordination, and the correlation significance for each topographic metric to the distribution of HPUs in the ordination space was examined ($p = 0.05$).

Multinomial Logistic Regression Model Development

A logistic regression approach was used to probabilistically model HPUs using topographic independent variables (e.g., Kempen et al., 2009). Relationships between topographic metrics and soil type are often nonlinear, yet logistic regression models are suitable linear models for handling nonlinear relationships, particularly when the dependent variable is the probability of presence (Bailey et al., 2003b).

In a logistic regression model for predicting membership in various HPUs, the dependent (response) variables, Y_i, are the HPUs, where $i = 1, ..., n$ and n is the total number of HPUs present. Response probabilities are denoted $p_1, ..., p_n$ and represent the probability of the occurrence of Y_i as p_i. Logistic regression relates the probability of occurrence in a group, e.g., p_1, to a set of predictor variables using the logit transformation to linearize the problem. Consider the following example for a binomial case of $n = 2$ groups:

$$\text{logit}(p_1) = \ln\left(\frac{p_1}{p_2}\right) = \ln\left(\frac{p_1}{1-p_1}\right) = \boldsymbol{\beta}\mathbf{X}' \quad [1]$$

where $\mathbf{X}$ is a vector of predictor variables and $\boldsymbol{\beta}$ is a vector of model coefficients. Equation [1] can be expressed as the odds ratio:

$$\frac{p_1}{1-p_1} = \exp(\boldsymbol{\beta}\mathbf{X}') \quad [2]$$

Equation [2] can be used to derive the response probability for Group 1:

$$p_1 = \frac{\exp(\boldsymbol{\beta}\mathbf{X}')}{1+\exp(\boldsymbol{\beta}\mathbf{X}')} \quad [3]$$

This binomial example can be expanded to describe multinomial situations with more than two outcomes ($n > 2$). In the case of this study, n HPUs correspond with a response variable with n outcomes, and the probability of occurrence for any of these outcomes i is determined as

$$p_i = \frac{\exp(\boldsymbol{\beta}_i\mathbf{X}'_i)}{\exp(\boldsymbol{\beta}_1\mathbf{X}'_1)+\exp(\boldsymbol{\beta}_2\mathbf{X}'_2)+...+\exp(\boldsymbol{\beta}_n\mathbf{X}'_n)} \quad [4]$$

So, for a given point on the landscape, the regression model provides a probability for HPU 1, HPU 2, HPU 3, HPU 4, and HPU 5, and the probability values sum to 1.

Logistic regression requires that a reference dependent variable be used to make comparisons with all other dependent variables. We selected typical podzols, the dominant soil in WS3, as the reference variable to which all other HPUs were compared. A final predictor model was selected based on a number of model quality indicators, including the Akaike information criterion (AIC) (Campling et al., 2002), McFadden's pseudo R^2, the log-likelihood ratio test (Kempen et al., 2009), and the significance ($p < 0.05$) of a topographic metric as an independent variable for at least one of the HPUs.

Although dozens of topographic metrics may be computed using a DEM, it was likely that only a few were necessary to predict HPU distribution. Furthermore, the logistic regression model may have been limited by multicollinearity or failed to achieve model convergence if too many topographic metrics were used as predictor variables. The strongest correlations (positive and/or negative) between topographic metrics and NMS dimensions, as well as metric uniqueness in NMS space, were used to identify candidate topographic metrics for multinomial logistic regression (MNR). Combinations of candidate topographic metrics were systematically tested during MNR model development. First, a metric exhibiting strong correlation was tested alone. Then, a second metric with strong correlation in a different direction was added and the model was retested, until all possible models were assessed. The MNR models were evaluated using the aforementioned criteria (AIC, McFadden's pseudo R^2, and the log-likelihood ratio test). This process was repeated until all plausible models were assessed.

Validation Data Set and Model Accuracy

Two methods were used to assess model accuracy. Twenty-five percent of the total number of sites for each HPU ($n = 5$ E, 7 Bhs, 17 typical, and 9 Bh podzols) were randomly removed before model development for use as a validation data set. The mean prediction probability of each HPU validation data set was computed. Model accuracy was also assessed using error ma-

trices (Congalton and Green, 2008). Field-classified HPUs were compared with model predictions for probabilities ranging from 0.30 to 0.80 at intervals of 0.10 for a total of six matrices. Error matrices were used to interpret the overall accuracy—the number of field observations correctly classified by the model as a percentage of the total number of field observations. Overall accuracies, as well as the number of pedons captured by the model at a given probability threshold as a percentage of the total number of pedons considered, were computed for each error matrix and examined to determine the best model probability for predicting HPUs in WS3.

RESULTS

Hydropedologic Unit Ordination

Kruskal's stress criterion for the two-dimensional ordination was 0.20. Stress decreased to 0.12 with the addition of the third dimension. Kruskal's stress criterion values should be <0.2 to mitigate the risk of drawing false inferences (Clarke, 1993). Thus, a three-dimensional solution was used for this analysis. Examination of the NMS ordination of soil horizon presence and thickness data in the first two dimensions showed E, Bhs, typical, Bh, and bimodal podzols separated into groups (Fig. 4). The E, Bhs, typical, and Bh podzols also exhibited clustering in Dimensions 1 and 3, whereas bimodal podzols did not exhibit strong clustering (Fig. 4). Lengths of the vectors in Fig. 4 indicate Spearman correlation strength between the topographic metrics and the ordination dimensions. All correlations except PROF were significant in Dimension 1, only EDs, PLAN, and TPI correlations were significant in Dimension 2, and all correlations except elevation above stream (EAS), SLP, TWIs, TPI, and DI were significant in Dimension 3 ($p = 0.05$; Table 1). Overall, the strongest correlations for almost all topographic metrics occurred in Dimensions 1 and 3. Of the variables with the strongest correlations and greatest significance, EDb, both TWI variants, and UAA were positively correlated with the Bh and bimodal podzols and negatively correlated with the E, Bhs, and typical podzols (Fig. 4). The UAAb, EDs, FDs, Elev, and TPI metrics were positively correlated with E, Bhs, and typical podzols and negatively correlated with Bh and bimodal podzols (Table 1; Fig. 4).

Multinomial Logistic Regression and Predicted Soil Spatial Patterns

Bimodal podzols were excluded from MNR model development because of weak clustering in the ordination space and limited correlation with topographic metrics. After 25% of E podzol complex, Bhs, typical, and Bh podzols were removed for model validation, a total of 116 pedons remained for model development. The subset of topographic metrics that produced the best logistic regression model (the lowest AIC and highest R^2) included TWId, EDb, UAAb, and TPI. This model had an AIC of 157 and a McFadden's pseudo R^2 of 0.55 (log-likelihood ratio test statistic = 166, degrees of freedom = 12, $p < 0.001$). Table 2 provides MNR model output for the best subset model. The TWId metric was significant for predicting Bh podzols, EDb was significant for predicting E and Bhs podzols, UAAb was significant for predicting Bhs podzols, and TPI was significant for predicting Bh podzols ($p = 0.05$). The odds ratio represents the likelihood of a given HPU compared with the reference soil group, the typical podzol, predicted by a given topographic metric for every one-unit increase in metric value. For example, for each 1-m increase in EDb, there is an associated 79% decrease in

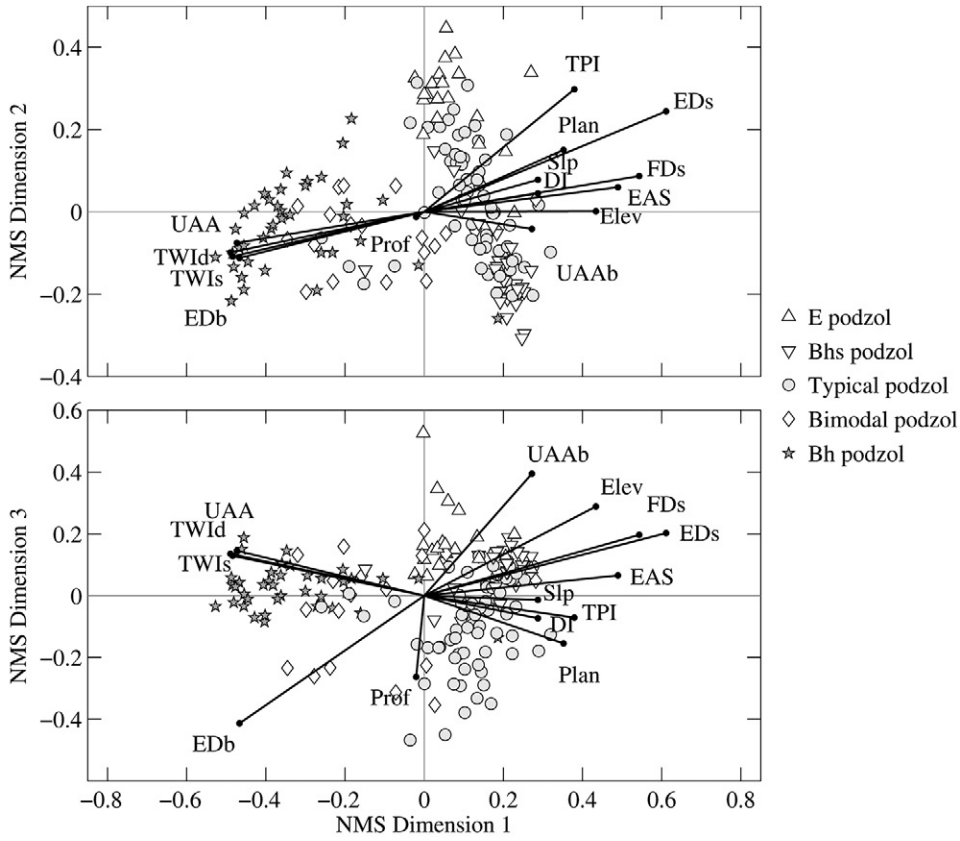

Fig. 4. Nonmetric multidimensional scaling (NMS) ordination using the Bray–Curtis dissimilarity with topographic metrics overlain as Spearman correlates demonstrated hydropedologic unit similarity through clustering in NMS space. Topographic metrics are downslope index (DI), elevation above stream (EAS), Euclidean distance from bedrock outcropping (EDb), Euclidean distance from stream (EDs), elevation (Elev), flow distance from stream (FDs), planform curvature (Plan), profile curvature (Prof), slope (Slp), topographic position index (TPI), topographic wetness index using DI (TWId), topographic wetness index using Slp (TWIs), upslope accumulated area (UAA), and bedrock-weighted upslope accumulated area (UAAb). Bimodal podzols did not cluster in Dimensions 1 and 3, which produced the lowest Kruskal's stress criterion, and were therefore excluded from multinomial logistic regression model development.

Table 2. Multinomial logistic regression model output for the best set of predictor topographic metrics, which included the topographic wetness index using the downslope index for the tanb parameter (TWId), Euclidean distance from bedrock outcropping (EDb), bedrock-weighted upslope accumulated area (UAAb), and the topographic position index (TPI). Beta values are the model coefficients, SE is the standard error of the coefficient, *t* is the *t*-statistic for the coefficient, and the *p* value is the probability. The odds ratio represents the likelihood of a given soil type compared with the baseline soil type (typical podzols) when a given topographic metric is used for prediction. Model selection criteria included Akaike information criterion = 157, McFadden's R^2 = 0.55, and log-likelihood ratio statistic = 166.

Soil type	Predictor	β	SE	*t*	*p*	Odds ratio
E complex	TWId	0.345	0.600	0.575	0.566	1.412
	EDb	−0.188	0.047	−3.998	0.000	0.790
	UAAb	4.302	3.355	1.282	0.200	2.578
	TPI	0.0850	0.1853	0.4586	0.6465	1.089
Bhs podzols	TWId	0.5380	0.570	0.943	0.345	1.713
	EDb	−0.071	0.028	−2.538	0.011	0.931
	UAAb	7.706	3.469	2.221	0.026	2221
	TPI	−0.052	0.200	−0.262	0.793	0.9489
Bh podzols	TWId	0.922	0.287	3.212	0.001	2.514
	EDb	0.003	0.007	0.365	0.715	1.003
	UAAb	−0.548	3.317	−0.165	0.869	0.578
	TPI	−0.567	0.193	−2.942	0.003	0.567

the likelihood, compared with the typical podzol, that the HPU present will be an E podzol.

Graphical representation of HPU probabilities based on topographic metrics aids in conceptualization of the odds ratios (Fig. 5). Each metric did not necessarily predict a probability of occurrence for the four HPUs included in the MNR model (e.g., TPI was not useful for predicting E or Bhs podzols). Hydropedologic unit graphical probability representations for each topographic metric are based on holding other metrics in the model at their mean values. For example, E-complex or Bhs podzols were more likely to occur with low EDb, indicating that proximity to bedrock outcrops was important for those HPUs. However, with increasing distance from bedrock, the soil is probably a typical or Bh podzol. Probability curves for TWId indicated that for lower TWId values soils are more likely to be typical podzols, and with increasing TWId soils are more likely to be Bh podzols. The UAAb was best suited for predicting typical and Bh podzols. Negative TPI values were associated with Bh podzols, whereas positive TPI values were associated typical podzols.

Model coefficients (β values; see Eq. [1] and [2]) from the MNR model were used to create probabilistic maps for the spatial distribution of HPUs in WS3 (Fig. 6). The E-complex and Bhs podzols were predicted to occur only in the region of the catchment with a bedrock-controlled landscape. The Bh podzols were predicted with the highest probability to occur near streams, with lower a probability of occurrence in less steep areas near the catchment divide and no probability elsewhere. Typical podzols were predicted to occur primarily in backslope positions. Predictor variables that included flow accumulation components (i.e., TWId and UAAb) created a network-like structure in the distribution of podzols across the catchment.

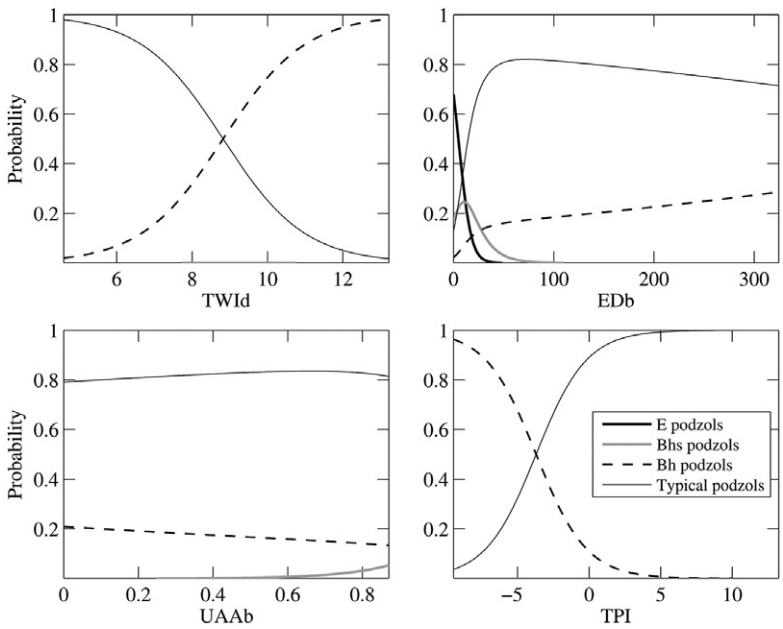

Fig. 5. Multinomial logistic regression (MNR) probabilities for E, Bhs, typical, and Bh podzols predicted by the topographic wetness index using the downslope index (TWId), Euclidean distance from bedrock outcropping (EDb), bedrock-weighted upslope accumulated area (UAAb), and the topographic position index (TPI). Bimodal podzols were not included in the MNR because nonmetric multidimensional (NMS) scaling ordination indicated that they were not well correlated with any topographic metrics in the most important NMS dimensions. Each metric did not necessarily predict a probability of occurrence for the four hydropedologic units included in the MNR model (e.g., TPI was not useful for predicting E or Bhs podzols).

Model Validation and Measures of Categorical Accuracy

Thirty-eight validation pedons, representing 25% of the total number of pedons (excluding bimodal podzols), were used for model validation. Typical podzol validation pedons achieved a mean prediction probability of 0.72 with a standard error (SE) of ±0.07, E-complex validation pedons achieved a mean of 0.42 (SE ± 0.08), Bhs podzol validation pedons achieved a mean of 0.51 (SE ± 0.09), and Bh podzol validation pedons achieved a mean of 0.54 (SE ± 0.13) (Fig. 7).

In general, as the model prediction probability increased, the overall model accuracy also increased but the number of pedons captured decreased (Fig. 8). Maximization of accuracy and the number of pedons classified by the model occurred at a probability of about 0.60 (Table 3). Overall model accuracy at the 0.60 prediction probability value, determined by dividing the sum of all true positives by the total number of pedons in the error matrix, was 0.80. Note that 45 of the 154 pedons used for MNR model development failed to achieve probability ≥0.60 for any podzol type and thus were not included in the error matrix.

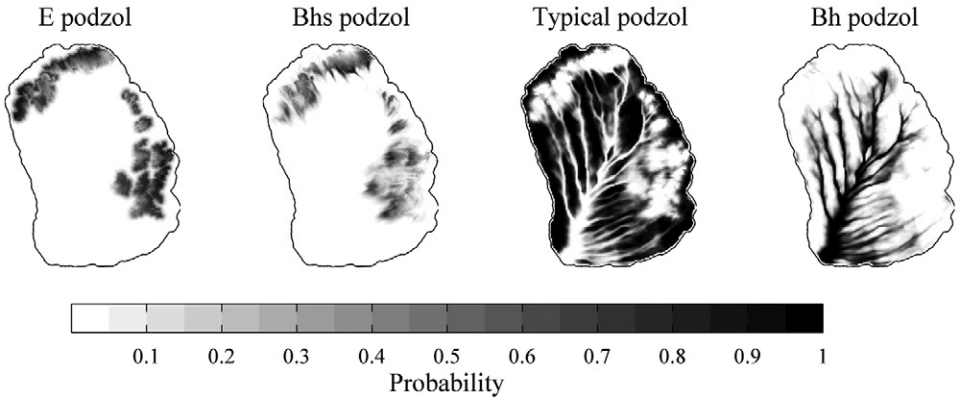

Fig. 6. Probabilistic hydropedologic soil maps of Watershed 3 for E, Bhs, typical, and Bh podzols.

DISCUSSION

Nonmetric Multidimensional Scaling Ordination Indicated Clustering of Most Hydropedologic Units

We expected HPUs to cluster in the NMS ordination based on the tendency for each to exhibit characteristic morphological attributes related to the presence and thickness of genetic horizons. For instance, E podzols are comprised of a thick eluviated horizon with or without a thin Bhs horizon over bedrock, while Bh podzols develop thick Bh horizons dominating most of the solum. Indeed, the similarity of horizon presence and thickness for each podzol type is reflected in the grouping indicated by the NMS ordination, suggesting that the HPUs serve as viable and distinct groups.

Bimodal podzols proved somewhat of an exception to clustering in the NMS ordination, exhibiting weak clustering in Dimensions 1 and 2 but no clustering in Dimensions 1 and 3. While this group exhibits a characteristic horizon sequence of an anomalously dark Bh horizon at the base of the solum, it is perhaps the most variable in terms of the thickness of horizons. Although occurring most frequently in near-stream areas, bimodal podzols can also be found away from streams at hillslope benches where water tables develop in the lower solum seasonally and persist for several weeks or longer (Bailey et al., 2014). Furthermore, field investigations indicated that although bimodal podzols represent a transition between typical and Bh podzols, the width of the transition is variable and often narrow, in some cases occurring across a few meters. Thus, bimodal podzol distribution may be visualized as a linear feature at the boundary between typical and Bh podzols, and their expected location can be interpreted from the MNR model results by finding areas where typical podzols transition to Bh podzols on the probability map (Fig. 6).

It was anticipated that UAAb and EDb would be useful for predicting E and Bhs podzols because these HPUs are always found immediately downslope of outcroppings or shallow-to-bedrock areas. The UAAb and EDb metrics were also useful for predicting typical and Bh podzols, which are more likely to occur farther away from outcrops and tend to have a smaller proportion of their upslope area in the bedrock-controlled landscape. The TWI proved a valuable metric for predicting typical and Bh podzols. This was expected because soil physical properties such as horizon thickness have been correlated with TWI in previous studies (e.g., Seibert et al., 2007). Both TWI variants exhibited strong correlations with HPU clustering in the NMS, but MNR results indicated that TWId was a better predictor than TWIs. The TPI was most useful for predicting Bh podzols that tend to occur on footslopes or toeslopes and typical podzols that tend to occur on backslopes. Our analysis did not find TWI or TPI useful for predicting E or Bhs podzols, probably because formation of these HPUs is most influenced by bedrock-controlled landscapes and less influenced by changes in slope or upslope area.

Profile curvature exhibited the second-weakest correlation with podzol groupings in NMS Dimension 2 and was the only topographic metric that failed to achieve a significant correlation in Dimension 1 (p = 0.88 and 0.86, respectively). Previous researchers reported that profile curvature is a primary geomorphic parameter important for understanding surface processes (Schmidt et al., 2003). However, previous analyses finding the importance of curvature utilized DEMs of 10-m resolution or coarser. This study suggests that the importance of profile curvature may be less when using DEMs of resolutions finer than 10 m or for mapping of soils in a hydrologic context. Application across broader or more topographically diverse areas than our

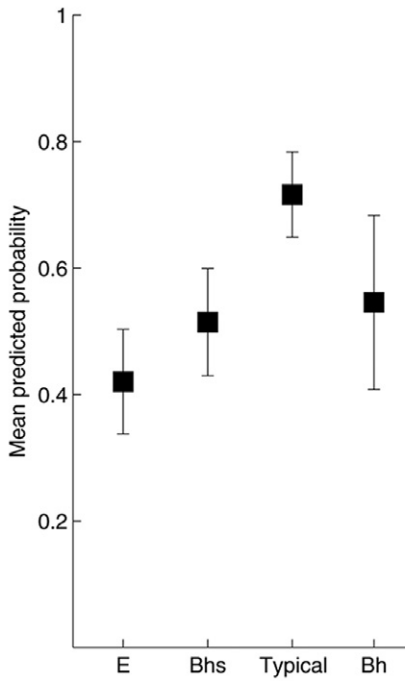

Fig. 7. Mean probability and standard error for each set of validation hydropedologic unit pedons. Validation pedons were excluded during multinomial logistic regression model development.

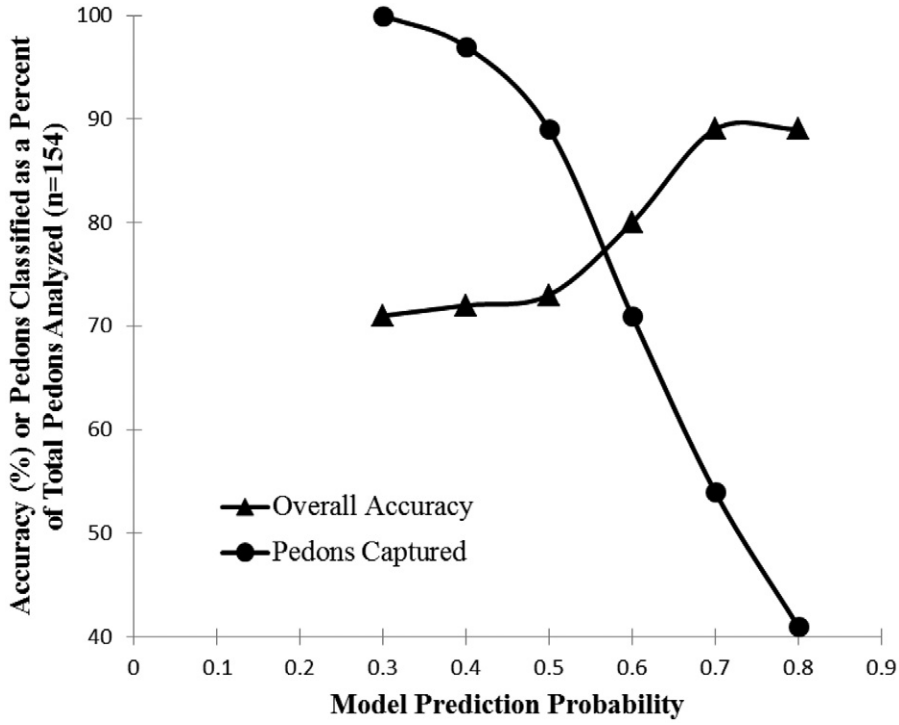

Fig. 8. Multinomial logistic regression model accuracy was assessed using error matrices comparing hydropedologic units (HPUs) identified in the field with those classified by the logistic regression model across a range of prediction probabilities. The resulting categorical accuracy values, as well as the number of pedons captured by the model as a percentage of the total pedons considered, were examined in a scatterplot. The best model probability for predicting HPUs in Watershed 3 occurs when accuracy measures and number of pedons captured are maximized (i.e., where the curves intersect).

study area may find this metric to be more useful. In WS3, two contrasting groups, E podzols and typical podzols, both show the full range in profile curvature seen for all five HPUs considered (Bailey et al., 2014).

Predicted Soil Spatial Patterns and Soil Development

In general, HPU predictions matched field observations and the current understanding of pedogenic and hydrologic spatial variation in WS3. The E podzols were predicted near bedrock, Bhs podzols were predicted downslope of E podzols, Bh podzols were predicted adjacent to streams, and typical podzols were predicted everywhere else (Fig. 6). Bimodal podzols were excluded during model development but can be interpreted to occur at the typical–Bh podzol transition zone.

Variation in the predicted probabilities among HPUs (Fig. 7) has several possible explanations. Multinomial logistic regression (MNR) can be biased by a disproportionate number of samples between groups (Real et al., 2006). In WS3, typical podzols are the dominant HPU and represent the largest number of pedons in the sample data set used to develop the MNR model (followed by Bh, Bhs, and finally E-complex). The uneven number of samples has the potential to bias model predictions toward HPUs with more samples. This may explain why typical and Bh podzols had a higher mean prediction probability than E or Bhs podzols. Furthermore, the E and Bhs podzol extent is more variable than the more prevalent (typical podzols) or less variable (Bh podzols) soil units. Thus, it can be expected that the accuracy of their prediction will be somewhat lower. Finally, since the occurrence of E and Bhs podzols is always associated with bedrock-controlled landscapes, the predictive capability of the MNR model is limited by the accuracy of the bedrock outcrop map.

Five field-identified Bh podzols located ≥20 m from the nearest mapped stream occurred in the southeast portion of the catchment where stream channels are poorly defined or absent, yet digital terrain analyses indicated high TWIs, TWId, and UAA values. These Bh podzols occurred on slopes of 10 to 20%, which is less steep than most slopes in WS3 but generally similar to slopes in near-stream areas. In this region, four of five Bh podzols found away from streams were correctly mapped. The pedogenesis of Bh podzols is hypothesized to be related to lateral subsurface flow processes and the development of more persistent water tables, which frequently saturate much of the solum (Bailey et al., 2014; Gannon et al., 2014). Typically, such conditions are found within 5 to 10 m of a stream in areas that remain saturated for longer periods following storm events or during the non-growing season. These hillslope Bh podzols appear to be associated with low slope benches with larger UAA or TWI values and could also be influenced by zones of lower parent material conductivity. Gannon et al. (2014) distinguished hillslope and near-stream Bh podzols as separate HPUs based on greater and more frequent variation in water table depth in the hillslope variant.

The utility of mapping soils by HPUs can be illustrated by combining the individual probabilistic maps from MNR (Fig. 6)

Table 3. Error matrix for the multinomial logistic regression model with a prediction probability threshold of 0.60. Reference data refers to field observations and classified data refers to model predictions. Values indicate agreement or disagreement between field observations and model predictions. For instance, 48 pits identified as typical podzols in the field were also classified as typical podzols by the model, but six were incorrectly classified as Bh podzols. Overall accuracy (sum of correctly mapped hydropedologic units [HPUs] divided by the sum of total mapped HPUs) was 80%, and 71% of the pedons were captured.

Classified data	Reference data (field)				
(mapped)	Typical	E	Bhs	Bh	Total
Typical	48	0	0	9	57
E	0	7	1	0	8
Bhs	3	3	11	0	17
Bh	6	0	0	21	27
Total	57	10	12	30	

into a single map based on the one soil unit with >40% occurrence in each grid cell (Fig. 9). This approach chooses a single most likely soil unit for each cell while leaving very few cells unclassified. Such a map provides a spatial representation of the translocational catena proposed by Bailey et al. (2014) to explain patterns of podzolization at HBEF and shown by Bourgault et al. (2015) to describe differences in the color, morphology, and chemistry of spodic horizons. The map highlights regions dominated by lateral eluviation or lateral illuviation and shows that only about half the catchment is dominated by podzolization processes occurring under vertical percolation at the pedon scale. The E podzols represent portions of the landscape where lateral eluviation is a dominant pedogenic process. This agrees with Zimmer et al. (2013), who showed that concentrations of Al and dissolved organic C were elevated in the groundwater in this soil unit. The Bhs and Bh podzols indicate portions of the catchment where lateral illuviation is a dominant pedogenic process, which is reflected by a broader depth distribution of C through the soil profile (Bailey et al., 2014).

Development of this HPU map (Fig. 9) differs from previous applications of hydropedologic concepts to define map units (Lin et al., 2008; Zhu et al., 2013) in that it does not build on existing high-intensity soil surveys. Thus, none of the expert delineation of soil polygons typical to soil survey went into its development. Rather, it is simply based on a statistical analysis, via the NMS and MNR, of relationships between topographic and bedrock metrics and soil horizonation patterns. Thus, the statistical development acts as an objective test of the validity of the HPUs as distinct soil groups and of their predictability based on landscape position. Furthermore, independence from established soil series highlights the distinctness of the HPUs from previously established map units. In our study area, soil series in shallow to bedrock landscapes are the Lyman and Tunbridge series, considered to be somewhat excessively to well drained. The hydropedologic approach taken by this study illuminates that bedrock-controlled portions of this region may be characterized by less well drained conditions, with the water table extending well into the solum on nearly an event basis. Such contrasts in drainage may have important implications for the management and understanding of the biogeochemistry of these landscapes.

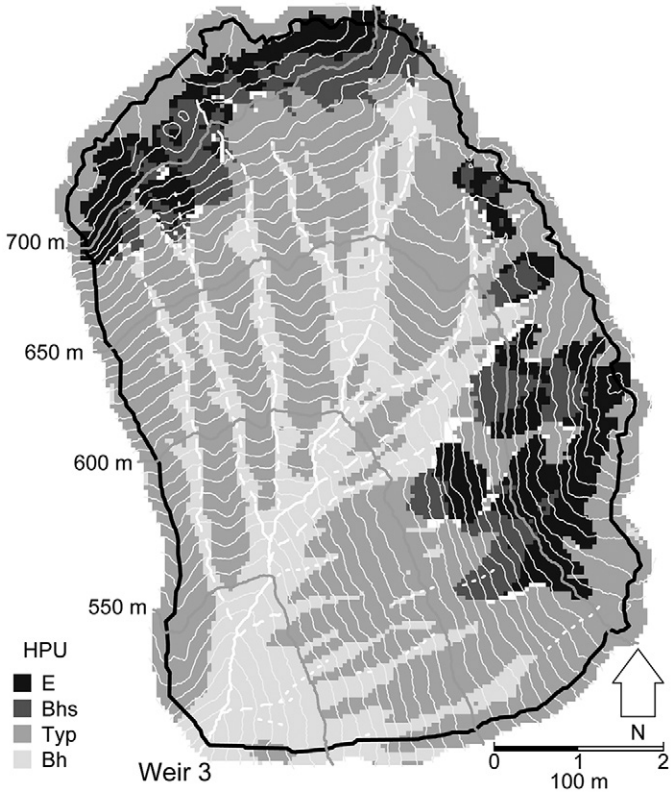

Fig. 9. Map of hydropedologic units (HPUs) of Watershed 3 derived from classifying each cell by the unit most likely to occur in the multinomial logistic regression. Cells where no one HPU was predicted to have an occurrence of 40% or more remained unclassified and are shown as white cells. This map highlights differences in soil formation due to hydropedologic processes, including zones where lateral eluviation (E podzols) or lateral illuviation (Bhs and Bh podzols) vs. vertical podzolization (typical podzols) predominate.

Implications for Runoff Processes and Soil Carbon

In general, mapping the spatial distribution of soils defined as HPUs offers novel insights into subsurface hydrologic dynamics and biogeochemical processes. Areas that experience flashy water table incursions in the solum during storm events or snowmelt (E and Bhs podzols), areas that experience the development of seasonal to perennial water tables (Bh and bimodal podzols), and areas that follow the more traditional view of vertical unsaturated water percolation through the soil (typical podzols) all can be interpreted from the podzol distribution maps (Fig. 6 and 9). The spatial extent of HPUs that experience water tables in the B horizons for various periods of time challenges previous notions that these steep, upland, coarse-textured soils are well drained. Rather, these transient and seasonal water tables suggest sharp spatial gradients in drainage conditions. Gannon et al. (2014) found that subsurface flow was initiated at different threshold levels of combined catchment storage and event rainfall for different HPUs.

The ability to map these soils and identify when subsurface flow is occurring also suggests that runoff generation processes can be spatially predicted. Near-stream Bh podzols behave in a manner consistent with the classic concept of variable source areas, where water tables develop most quickly and frequently, directly leading to streamflow generation (Hewlett and Hibbert, 1967; Dunne et al., 1975). Bedrock-controlled landscapes more distal from stream networks have not been as well recognized as active streamflow generation areas. But frequent water table incursions in E and Bhs podzols and expansion of the ephemeral to intermittent portions of the drainage network during events suggest that these areas can act as contributing areas to runoff generation (Gannon et al., 2014).

Likewise, biogeochemical processes might be expected to vary with these HPUs. For example, Morse et al. (2014) found strong links between biogeochemical cycling and mineral soil C, suggesting that deeper C accumulation than is typically considered in biogeochemical studies may be an indicator of C and N

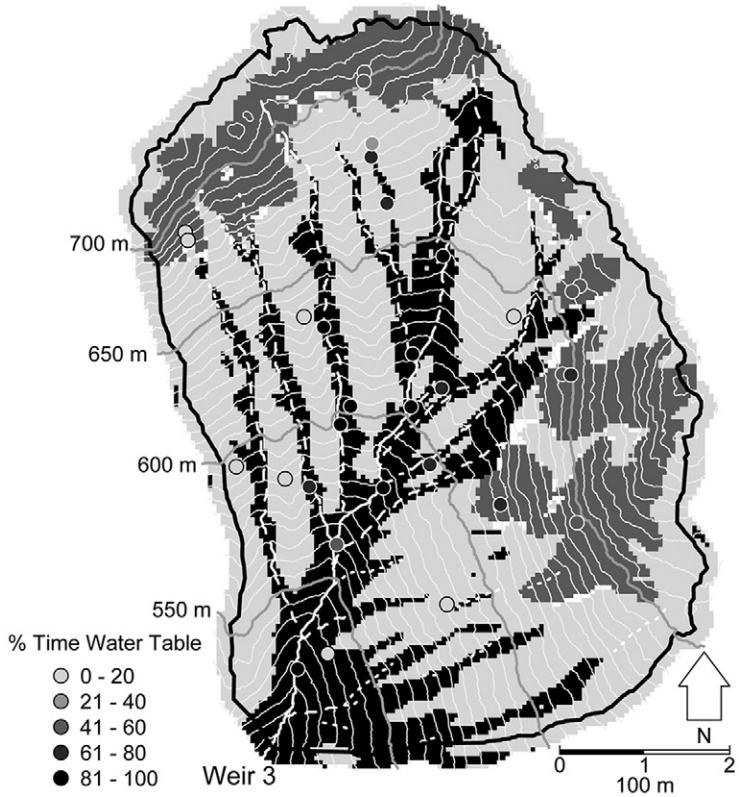

Fig. 10. Map of frequency of water table presence within the solum predicted by logistic regression analysis. White cells indicate areas where no one hydropedologic unit was predicted to have an occurrence of 40% or more and were unclassified. Circles represent measurements of the proportion of the time that the water table was detected above the B–C interface in wells monitored at 10-min intervals for a minimum of 3 yr (Gannon et al., 2104).

cycling capacity at the catchment scale. Wexler et al. (2014) found isotopic evidence for denitrification along intermittent portions of the stream network in WS3 during summer conditions when streamflow was not present but when water tables were still present in near-stream Bh podzols. Hydropedologic mapping (Fig. 10) of water table variations might provide a way to scale these observations to the catchment, suggesting the possibility for closing a long-standing gap in understanding of forest N cycles.

The soil maps (Fig. 6 and 9) generated from our model suggest a greater spatial extent of C-rich soils (Bh, bimodal, and Bhs podzols) in HBEF watersheds than indicated by previous studies (Huntington et al., 1988; Fahey et al., 2010), which has implications for soil C accounting and C fate in a changing climate. Bailey et al. (2014) provided average profile C content estimates for each of the HPUs in this study. Using the model presented here, their C content estimates, and a 40% probability threshold for HPU classification, the area-weighted average soil C estimate for WS3 is 20.0 ($\pm$3.6) kg m^{-2}. This is 27% greater than previously estimated for Hubbard Brook (Fahey et al., 2010) based on an unweighted mean of all soil samples collected. Thus, stratifying field samples and calculations based on HPUs may better capture the contribution of less common soil units to overall catchment C sequestration.

Long-term climate forecasts for New England have predicted that the region will experience a 3 to 5°C rise in temperature, increased evapotranspiration leading to as much as a 31% reduction in streamflow, and a decrease in the amount and duration of snow cover (Hayhoe et al., 2006; Campbell et al., 2011). These conditions will affect groundwater dynamics and may interact in complex ways to influence mineral soil C storage. This is particularly important because soils with higher C content in B horizons are associated with frequently saturated conditions (Bailey et al., 2014) in variable source areas of the catchment (Fig. 9 and 10). Laterally deposited spodic C has a distinct morphology and associated metal chemistry compared with vertically deposited spodic C (Bourgault et al., 2015). While these C stores might be considered to have been accumulated slowly and to be stable in the future, it is unknown whether a change in the hydrologic regime in these horizons might alter sequestration or destabilize storage in the future.

CONCLUSIONS

To gain a better understanding of the hydrologic and biogeochemical functioning of headwater catchments, we used a hydropedologic framework to map the distribution of soils using topographic and bedrock outcrop metrics as predictor variables in an MNR model. An ordination of soil horizon data using NMS indicated that the TWI, EDb, UAAb, and TPI exhibited the strongest correlations with HPU clustering. Our model indicated that in small headwater systems at HBEF, these four topographic metrics were well correlated to HPUs defined by the presence and thickness of genetic horizons.

While this analysis has been confined to a single headwater catchment, we suggest that the HPUs developed here may be typical of a much broader area of the northeastern United States and adjacent Canada where Spodosols dominate under the influence of cool humid conditions, forest vegetation, and relatively acidic, coarse-textured parent materials. Furthermore, landscapes dominated by mosaics of outcrops and shallow bedrock in steep upland positions are typical of a much broader area, suggesting the possibility of analogous variations in soil drainage and water table regime in similar settings but across a much broader range of soil orders.

Analysis of the spatial patterns of HPUs provides a better hydrologic and biogeochemical context and a more process-based understanding of the spatial heterogeneity of soil and land management characteristics than traditional soil map units, offering an important complement to taxonomically based surveys. Soil HPU probability maps offer information about the spatial distribution of soils that can be used to interpret hydrologic and biogeochemical function within a catchment. Subsurface flow paths, water table fluctuations, C storage in soils, and perhaps ecological communities and variations in productivity may be inferred from examination of the spatial pattern of HPUs.

ACKNOWLEDGMENTS

Financial support was provided by the National Science Foundation

(NSF) Long-Term Ecological Research (DEB 1114804), Hydrologic Sciences (EAR 1014507), and Research Experience for Undergraduate (DBI/EAR 0754678) programs. The LiDAR data were collected by Photo Science, Inc., for the White Mountain National Forest. Field work was partially conducted by Patricia Brousseau, Kaitland Harvey, Margaret Zimmer, Rebecca Bourgault, Margaret Burns, and Geoffrey Schwaner. The Hubbard Brook Experimental Forest is operated and maintained by the US Forest Service, Northern Research Station, Newtown Square, PA, and is part of the NSF Long-Term Ecological Research network.

REFERENCES

Bailey, A.S., J.W. Hornbeck, J.L. Campbell, and C. Eagar. 2003a. Hydrometeorological database for Hubbard Brook Experimental Forest: 1955–2000. US For. Serv., Northeast. Res. Stn., Newtown Square, PA.

Bailey, N., T. Clements, J.T. Lee, and S. Thompson. 2003b. Modelling soil series data to facilitate targeted habitat restoration: A polytomous logistic regression approach. J. Environ. Manage. 67:395–407. doi:10.1016/S0301-4797(02)00227-X

Bailey, S.W., P.A. Brousseau, K.J. McGuire, and D.S. Ross. 2014. Influence of landscape position and transient water table on soil development and carbon distribution in a steep, headwater catchment. Geoderma 226-227:279–289. doi:10.1016/j.geoderma.2014.02.017

Bailey, S.W., D.C. Buso, and G.E. Likens. 2003c. Implications of sodium mass balance for interpreting the calcium cycle of a forested ecosystem. Ecology 84:471–484. doi:10.1890/0012-9658(2003)084[0471:IOSMBF]2.0.CO;2

Barton, C.C., R.H. Camerlo, and S.W. Bailey. 1997. Bedrock geologic map of Hubbard Brook Experimental Forest and maps of fractures and geology in roadcuts along Interstate-93, Grafton County, New Hampshire. Sheet 1, Scale 1:12,000; Sheet 002, Scale 001:200. Misc. Invest. Ser. Map I-2562. USGS, Reston, VA.

Beven, K., and M. Kirkby. 1979. A physically based, variable contributing area model of basin hydrology. Hydrol. Sci. Bull. 24:43–69. doi:10.1080/02626667909491834

Boettinger, J.L., D. Howell, A. Moore, A.E. Hartemink, and S. Kienast-Brown. 2010. Digital soil mapping: Bridging Research, environmental application, and operation. Progr. Soil Sci. 2. Springer-Verlag, Dordrecht, the Netherlands.

Bourgault, R.R., D.S. Ross, and S.W. Bailey. 2015. Chemical and morphological distinctions between vertically and laterally developed spodic horizons at Hubbard Brook. Soil Sci. Soc. Am. J. 79:XXX–XXX (this issue). doi:10.2136/sssaj2014.05.0190

Bray, J.R., and J.T. Curtis. 1957. An ordination of upland forest communities of southern Wisconsin. Ecol. Monogr. 27:325–349. doi:10.2307/1942268

Brown, D.J., M.K. Clayton, and K. McSweeney. 2004. Potential terrain controls on soil color, texture contrast and grain-size deposition for the original catena landscape in Uganda. Geoderma 122:51–72. doi:10.1016/j.geoderma.2003.12.004

Bushnell, T.M. 1943. Some aspects of the soil catena concept. Soil Sci. Soc. Am. J. 7:466–476. doi:10.2136/sssaj1943.036159950007000C0079x

Campbell, J.L., C.T. Driscoll, A. Pourmokhtarian, and K. Hayhoe. 2011. Streamflow responses to past and projected future changes in climate at the Hubbard Brook Experimental Forest, New Hampshire, United States. Water Resour. Res. 47:W02514. doi:10.1029/2010WR009438

Campling, P., A. Gobin, and J. Feyen. 2002. Logistic modeling to spatially predict the probability of soil drainage classes. Soil Sci. Soc. Am. J. 66:1390–1401. doi:10.2136/sssaj2002.1390

Clarke, K.R. 1993. Non-parametric multivariate analyses of changes in community structure. Aust. J. Ecol. 18:117–143. doi:10.1111/j.1442-9993.1993.tb00438.x

Congalton, R.G., and K. Green. 2008. Assessing the accuracy of remotely sensed data: Principles and practices. 2nd ed. CRC Press, Boca Raton, FL.

Conrad, O. 2011. System for Automated Geoscientific Analyses Version 2.1.0. http://www.saga-gis.org/en/index.html

Debella-Gilo, M., and B. Etzelmüller. 2009. Spatial prediction of soil classes using digital terrain analysis and multinomial logistic regression modeling integrated in GIS: Examples from Vestfold County, Norway. Catena 77:8–18. doi:10.1016/j.catena.2008.12.001

Detty, J.M., and K.J. McGuire. 2010. Threshold changes in storm runoff generation at a till-mantled headwater catchment. Water Resour. Res. 46:W07525. doi:10.1029/2009WR008102

Dunne, T., T. Moore, and C. Taylor. 1975. Recognition and prediction of runoff-producing zones in humid regions. Hydrol. Sci. Bull. 20:305–327.

Fahey, T.J., P.B. Woodbury, J.J. Battles, C.L. Goodale, S.P. Hamburg, S.V. Ollinger, and C.W. Woodall. 2010. Forest carbon storage: Ecology, management, and policy. Front. Ecol. Environ. 8:245–252. doi:10.1890/080169

Faith, D.P., P.R. Minchin, and L. Belbin. 1987. Compositional dissimilarity as a robust measure of ecological distance. Vegetatio 69:57–68. doi:10.1007/BF00038687

Gannon, J.P., S.W. Bailey, and K.J. McGuire. 2014. Organizing groundwater regimes and response thresholds by soils: A framework for understanding runoff generation in a headwater catchment. Water Resour. Res. 50:8403–8419. doi:10.1002/2014WR015498

Gessler, P.E., O.A. Chadwick, F. Chamran, L. Althouse, and K. Holmes. 2000. Modeling soil-landscape and ecosystem properties using terrain attributes. Soil Sci. Soc. Am. J. 64:2046–2056. doi:10.2136/sssaj2000.6462046x

Gillin, C.P., K.J. McGuire, S.W. Bailey, and S.P. Prisley. 2015. Evaluation of LiDAR-derived DEMs through terrain analysis and field comparison. Photogramm. Eng. Remote Sens. (in press).

Guisan, A., S.B. Weiss, and A.D. Weiss. 1999. GLM versus CCA spatial modeling of plant species distribution. Plant Ecol. 143:107–122. doi:10.1023/A:1009841519580

Guntner, A., J. Seibert, and S. Uhlenbrook. 2004. Modeling spatial patterns of saturated areas: An evaluation of different terrain indices. Water Resour. Res. 40:W05114. doi:10.1029/2003WR002864

Hayhoe, K., C.P. Wake, T.G. Huntington, L. Luo, M.D. Schwartz, J. Sheffield, et al. 2006. Past and future changes in climate and hydrological indicators in the US Northeast. Clim. Dyn. 28:381–407. doi:10.1007/s00382-006-0187-8

Hewlett, J.D., and A.R. Hibbert. 1967. Factors affecting the response of small watersheds to precipitation in humid areas. In: W.E. Sopper and H.W. Lull, editors, International Symposium on Forest Hydrology, University Park, PA. 29 Aug.–10 Sept. 1965. Pergamon Press, New York. p. 275–291.

Hjerdt, K.N. 2004. A new topographic index to quantify downslope controls on local drainage. Water Resour. Res. 40:W05602. doi:10.1029/2004wr003130

Homer, J.W. 1999. Soil survey of Grafton County Area, New Hampshire. US Gov. Print. Office, Washington, DC.

Huntington, T.G., D.F. Ryan, and S.P. Hamburg. 1988. Estimating soil nitrogen and carbon pools in a northern hardwood forest ecosystem. Soil Sci. Soc. Am. J. 52:1162–1167. doi:10.2136/sssaj1988.03615995005200040049x

Jankowski, M. 2013. The evidence of lateral podzolization in sandy soils of northern Poland. Catena 112:139–147. doi:10.1016/j.catena.2013.03.013

Jenny, H. 1941. Factors of soil formation: A System of quantitative pedology. McGraw-Hill, New York.

Johnson, C.E., C.T. Driscoll, T.G. Siccama, and G.E. Likens. 2000. Element fluxes and landscape position in a northern hardwood forest watershed ecosystem. Ecosystems 3:159–184. doi:10.1007/s100210000017

Kempen, B., D. Brus, G. Heuvelink, and J. Stoorvogel. 2009. Updating the 1:50,000 Dutch soil map using legacy soil data: A multinomial logistic regression approach. Geoderma 151:311–326. doi:10.1016/j.geoderma.2009.04.023

Lagacherie, P., A. McBratney, and M. Voltz. 2006. Digital soil mapping: An introductory perspective. Dev. Soil Sci. 31. Elsevier, Amsterdam.

Likens, G.E. 2013. Biogeochemistry of a forested ecosystem. 3rd ed. Springer, New York.

Likens, G.E., and D.C. Buso. 2006. Variation in streamwater chemistry throughout the Hubbard Brook valley. Biogeochemistry 78:1–30. doi:10.1007/s10533-005-2024-2

Lin, H.S., J. Bouma, Y. Pachepsky, A. Western, J. Thompson, R. van Genuchten, et al. 2006. Hydropedology: Synergistic integration of pedology and hydrology. Water Resour. Res. 42:W05301. doi:10.1029/2005WR004085

Lin, H.S., E. Brook, P.A. McDaniel, and J. Boll. 2008. Hydropedology and surface/subsurface runoff processes. In: Encyclopedia of hydrologic sciences. Part 10. Rainfall–runoff processes. John Wiley & Sons, Ltd., Chichester, UK. doi:10.1002/0470848944.hsa306

McDaniel, P.A., G.R. Bathke, S.W. Buol, D.K. Cassel, and A.L. Falen. 1992. Secondary manganese/iron ratios as pedochemical indicators of field-scale throughflow water movement. Soil Sci. Soc. Am. J. 56:1211–1217. doi:10.2136/sssaj1992.03615995005600040034x

McDonnell, J.J., M. Sivapalan, K. Vaché, S. Dunn, G. Grant, R. Haggerty,

et al. 2007. Moving beyond heterogeneity and process complexity: A new vision for watershed hydrology. Water Resour. Res. 43:W07301. doi:10.1029/2006WR005467

McDowell, W.H., and T. Wood. 1984. Podzolization: Soil processes control dissolved organic carbon concentrations in stream water. Soil Sci. 137:23–32. doi:10.1097/00010694-198401000-00004

Merot, P., B. Ezzahar, C. Walter, and P. Aurousseau. 1995. Mapping waterlogging of soils using digital terrain models. Hydrol. Processes 9:27–34. doi:10.1002/hyp.3360090104

Moore, I.D., P.E. Gessler, G.A. Nielsen, and G.A. Petersen. 1993. Soil attribute prediction using terrain analysis. Soil Sci. Soc. Am. J. 57:443–452. doi:10.2136/sssaj1993.03615995005700020026x

Morse, J.L., S.F. Werner, C.P. Gillin, C.L. Goodale, S.W. Bailey, K.J. McGuire, et al. 2014. Searching for biogeochemical hotspots in three dimensions: Soil C and N cycling in hydropedologic settings in a northern hardwood forest. J. Geophys. Res. Biogeosci. 119:1596–1607. doi:10.1002/2013JG002589.

Palmer, S.M., C.T. Driscoll, and C.E. Johnson. 2004. Long-term trends in soil solution and stream water chemistry at the Hubbard Brook Experimental Forest: Relationship with landscape position. Biogeochemistry 68:51–70. doi:10.1023/B:BIOG.0000025741.88474.0d

Park, S.J., and T.P. Burt. 2002. Identification and characterization of pedogeomorphological processes on a hillslope. Soil Sci. Soc. Am. J. 66:1897–1910. doi:10.2136/sssaj2002.1897

Pennock, D.J., B.J. Zebarth, and E. De Jong. 1987. Landform classification and soil distribution in hummocky terrain, Saskatchewan, Canada. Geoderma 40:297–315. doi:10.1016/0016-7061(87)90040-1

Real, R., A.M. Barbosa, and J.M. Vargas. 2006. Obtaining environmental favourability functions from logistic regression. Environ. Ecol. Stat. 13:237–245. doi:10.1007/s10651-005-0003-3

Schmidt, J., I. Evans, and J. Brinkmann. 2003. Comparison of polynomial models for land surface curvature calculation. Int. J. Geogr. Inf. Sci. 17:797–814. doi:10.1080/1365881031000159605 8

Seibert, J., and B.L. McGlynn. 2007. A new triangular multiple flow direction algorithm for computing upslope areas from gridded digital elevation models. Water Resour. Res. 43:W04501. doi:10.1029/2006WR005128

Seibert, J., J. Stendahl, and R. Sørensen. 2007. Topographical influences on soil properties in boreal forests. Geoderma 141:139–148. doi:10.1016/j.geoderma.2007.05.013

Siccama, T.G., T.J. Fahey, C.E. Johnson, T.W. Sherry, E.G. Denny, E.B. Girdler, et al. 2007. Population and biomass dynamics in a northern hardwood forest at Hubbard Brook. Can. J. For. Res. 37:737–749. doi:10.1139/X06-261

Sommer, M., D. Halm, U. Weller, M. Zarei, and K. Stahr. 2000. Lateral podzolization in a granite landscape. Soil Sci. Soc. Am. J. 64:1434–1442. doi:10.2136/sssaj2000.6441434x

Sommer, M., and E. Schlichting. 1997. Archetypes of catenas in respect to matter: A concept for structuring and grouping catenas. Geoderma 76:1–33. doi:10.1016/S0016-7061(96)00095-X

Travis, M.R., G.H. Elsner, W.D. Iverson, and C.G. Johnson. 1975. VIEWIT: Computation of seen areas, slope, and aspect for land-use planning. Gen. Tech. Rep. PSW-11/1975. US For. Serv., Berkeley, CA.

Wang, L., and H. Liu. 2006. An efficient method for identifying and filling surface depressions in digital elevation models for hydrologic analysis and modelling. Int. J. Geogr. Inf. Sci. 20:193–213. doi:10.1080/13658810500433453

Wexler, S.K., C.L. Goodale, K.J. McGuire, S.W. Bailey, and P.M. Groffman. 2014. Isotopic signals of summer denitrification in a northern hardwood forested catchment. Proc. Natl. Acad. Sci. 111:16413–16418. doi:10.1073/pnas.1404321111

Zaslavsky, D., and A.S. Rogowski. 1969. Hydrologic and morphologic implications of anisotropy and infiltration in soil profile development. Soil Sci. Soc. Am. Proc. 33:594–599. doi:10.2136/sssaj1969.03615995003300040031x

Zevenbergen, L.W., and C.R. Thorne. 1987. Quantitative analysis of land surface topography. Earth Surf. Processes Landforms 12:47–56. doi:10.1002/esp.3290120107

Zhu, Q., H.S. Lin, and J.A. Doolittle. 2013. Functional soil mapping for site-specific soil moisture and crop yield management. Geoderma 200-201:45–54. doi:10.1016/j.geoderma.2013.02.001

Zimmer, M.A., S.W. Bailey, K.J. McGuire, and T.D. Bullen. 2013. Fine scale variations of surface water chemistry in an ephemeral to perennial drainage network. Hydrol. Processes 27:3438–3451. doi:10.1002/hyp.9449